J. Fluid Mech. (1978), *vol.* 86, *part* 1, *pp.* 129–145
Printed in Great Britain

Extended Stokes series: laminar flow through a loosely coiled pipe

By MILTON VAN DYKE

Department of Mechanical Engineering, Stanford University, Stanford, California 94305

(Received 5 August 1976 and in revised form 2 June 1977)

Dean's series for steady fully developed laminar flow through a toroidal pipe of small curvature ratio has been extended by computer to 24 terms. Analysis suggests that convergence is limited by a square-root singularity on the negative axis of the square of the Dean number. An Euler transformation and extraction of the leading and secondary singularities at infinity render the series accurate for all Dean numbers. For curvature ratios no greater than $\frac{1}{250}$, experimental measurements of the laminar friction factor agree with the theory over a wide range of Dean numbers. In particular, they confirm our conclusion that the friction in a loosely coiled pipe grows asymptotically as the one-quarter power of the Dean number based on mean flow speed. This contradicts a number of incomplete boundary-layer analyses in the literature, which predict a square-root variation.

1. Introduction

An attractive alternative to finite-difference computation, at least in simple problems, consists of extending a perturbation series to high order by delegating to the computer the rapidly mounting arithmetic labour. Contemporary digital computers can, in a few minutes, calculate hundreds of terms for a linear problem and dozens of terms for a nonlinear one (Van Dyke 1975).

The range of applicability of the resulting series is ordinarily very limited. The author has discussed (Van Dyke 1974) how it can be extended by analysing the coefficients to unveil the analytic structure of the solution, and on that basis applying a variety of devices to improve the utility of the series. Most of these techniques are borrowed from physicists working on the statistical thermodynamics of critical phenomena (Gaunt & Guttmann 1974). Several additional ones are introduced in this paper.

A likely field of application for this three-step scheme of extension, analysis and improvement is to the solution of the Navier–Stokes equations. In particular, we consider here expansions for low Reynolds numbers. We understand *Reynolds number* in a generalized sense as any dimensionless measure of the relative importance of nonlinear and viscous effects, so that it may be the Rayleigh or Grashof number, Taylor number, etc., and in the present case the Dean number.

Such expansions have been termed *Stokes series*, because they are based on Stokes's investigation of the effect of viscosity on the motion of a pendulum, and on his linearized form of the Navier–Stokes equations. Of course Stokes and his successors discovered that for uniform flow past an object the low-Reynolds-number approximation is a singular perturbation. Since we do not know how to automate the method

of matched asymptotic expansions, we must restrict attention to regular perturbations: flows that are sufficiently confined by boundaries, or decay rapidly enough with distance. Then the solution of the Navier–Stokes equations is found as a power series in the Reynolds number.

For the linearized Oseen equations, the author has extended the Stokes series of Goldstein for the drag of a sphere to 24 terms (Van Dyke 1970), and found that from it can be extracted the drag at infinite Reynolds number. This raises the hope that likewise for the Navier–Stokes equations a Stokes series can be modified so as to converge for large Reynolds number. This objective might be thought unnecessarily ambitious, since high Reynolds numbers are the special province of boundary-layer theory. However, the laminar flows amenable to Stokes expansions are often just those where the boundary-layer structure is not clear because it involves colliding layers and internal jets, or the boundary-layer theory cannot be used at all because the flow separates. Furthermore, higher approximations in boundary-layer theory have proved disappointingly limited, and finite-difference computations become unreliable as the Reynolds number is increased. We see in this paper that the extended Stokes series provides, in a favourable problem, the most effective way of spanning the whole range of Reynolds numbers for laminar flow.

We examine one of the simplest problems that is realistic enough to have been the subject of experiments.† This is the steady fully developed laminar flow through a coiled pipe of circular cross-section. All previous analyses have been simplified by neglecting the helicity of the coil; furthermore Dean (1928) discovered that to a good approximation for loose coiling the motion depends not separately upon the Reynolds number R and the ratio a/L of the radius of the cross-section to the coiling radius, but only upon the product $R^2(a/L)$ – a similarity parameter that has subsequently, in several variants, been called the Dean number; we adopt both these approximations.

Previous work on this problem can be divided into four categories. First, experiments have been conducted by, among others, White (1929), Taylor (1929), Adler (1934), Itō (1959) and Mori & Nakayama (1965). Second, Dean (1927, 1928) developed a perturbation about Poiseuille flow through a straight pipe that yields the Stokes series being considered here, and carried it to the fourth power of the Dean number. Topakoglu (1967) retained higher-order terms in the curvature ratio a/L, to obtain a double power series in the curvature ratio and Dean number, as did Larrain & Bonilla (1970) in extending the series to 14th order by computer. Third, boundary-layer analyses for high Dean number have been proposed by Adler (1934), Barua (1963), Mori & Nakayama (1965), Itō (1969) and Smith (1975, 1976). Fourth, numerical solutions have been calculated by McConalogue & Srivastava (1968), Truesdell & Adler (1970), Akiyama & Cheng (1971), Austin & Seader (1973), Collins & Dennis (1975), and others. Truesdell & Adler and Austin & Seader include the effects of finite curvature ratio.

† The simplest problem of all is probably the steady plane flow inside a circle due to translation of the boundary with a speed that varies with angle, for which Kuwahara & Imai (1969) carried the Stokes series to eighth order by computer, and Conway (1978) carried it to 22nd order; but experiments would be difficult.

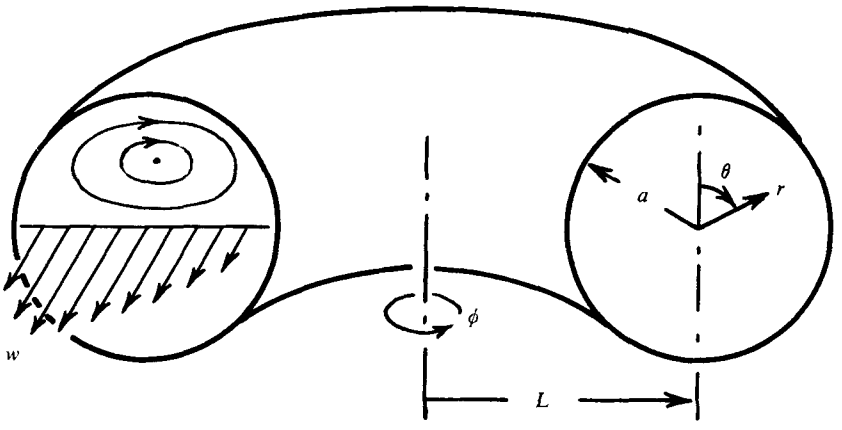

FIGURE 1. Notation for coiled pipe.

2. Summary of Dean's analysis

We adopt Dean's co-ordinate system (figure 1) and his normalization: lengths are referred to the radius a of the pipe, and the velocity w down the pipe to the maximum speed $W_0 = Ga^2/4\mu$ in a straight pipe under the same axial pressure gradient

$$G = L^{-1}\partial p/\partial\phi,$$

but the stream function ψ for the secondary motion is referred to the kinematic viscosity ν (which means that transverse velocities are referred to ν/a). Then in the approximations of negligible helicity and loose coiling the Navier–Stokes equations for incompressible fluid reduce to [Dean 1928, equations (15)–(18)]

$$\nabla^2 w = \frac{1}{r}\left(\frac{\partial\psi}{\partial r}\frac{\partial w}{\partial\theta} - \frac{\partial\psi}{\partial\theta}\frac{\partial w}{\partial r}\right) - 4, \tag{2.1}$$

$$\nabla^4\psi = \frac{1}{r}\left(\frac{\partial\psi}{\partial r}\frac{\partial}{\partial\theta} - \frac{\partial\psi}{\partial\theta}\frac{\partial}{\partial r}\right)\nabla^2\psi + Kw\left(\frac{\sin\theta}{r}\frac{\partial w}{\partial\theta} - \cos\theta\frac{\partial w}{\partial r}\right). \tag{2.2}$$

Here $\nabla^2 \equiv \partial^2/\partial r^2 + r^{-1}\partial/\partial r + r^{-2}\partial^2/\partial\theta^2$ is the Laplacian in the transverse plane, and K is Dean's similarity parameter

$$K = 2\left(\frac{W_0 a}{\nu}\right)^2\frac{a}{L} = \frac{G^2a^7}{8\mu^2\nu^2 L}. \tag{2.3}$$

The boundary conditions require that

$$w = \psi = \partial\psi/\partial r = 0 \quad \text{at} \quad r = 1. \tag{2.4}$$

If the pipe is straight, K is zero, and the solution is that for Poiseuille flow, with $w = w_0 \equiv 1 - r^2$ and $\psi = 0$. Dean treats the curved pipe as a systematic perturbation of the straight one by expanding in powers of K:

$$\left.\begin{aligned} w &= w_0 + Kw_1 + K^2 w_2 + \ldots, \\ \psi &= K\psi_1 + K^2\psi_2 + \ldots. \end{aligned}\right\} \tag{2.5}$$

Substituting into the equations and boundary conditions yields a sequence of successively more complicated linear problems that can be solved in turn to give

$$\left.\begin{aligned} \psi_1 &= \tfrac{1}{576}(4r - 9r^3 + 6r^5 - r^7)\cos\theta, \\ w_1 &= \tfrac{1}{576}(\tfrac{19}{40}r - r^3 + \tfrac{3}{4}r^5 - \tfrac{1}{4}r^7 + \tfrac{1}{40}r^9)\sin\theta, \end{aligned}\right\} \tag{2.6}$$

and so on. Dean quotes part of the solution for w_2, and then, remarking that 'the difficulty of successively finding the functions becomes rapidly greater', gives without details the result to order K^4 for the ratio of flux through the curved pipe to that through the corresponding straight pipe under the same pressure gradient:†

$$F_c/F_s = \sum_{n=0}^{\infty} a_n(\tfrac{1}{576}K)^{2n} = 1 - 0{\cdot}03058(\tfrac{1}{576}K)^2 + 0{\cdot}01195(\tfrac{1}{576}K)^4 + \dots . \tag{2.7}$$

Experimenters measure the *friction factor* λ and, following White (1929), usually plot the *friction ratio*, the resistance in the curved pipe divided by that in a straight pipe carrying the same flux. This is easily seen to be the reciprocal of the flux ratio (2.7), and is accordingly given in Dean's approximation by

$$\begin{aligned} \lambda_c/\lambda_s = (F_c/F_s)^{-1} &= \sum_{n=0}^{\infty} b_n(\tfrac{1}{576}K)^{2n} \\ &= 1 + 0{\cdot}03058(\tfrac{1}{576}K)^2 - 0{\cdot}01100(\tfrac{1}{576}K)^4 + \dots . \end{aligned} \tag{2.8}$$

In extending Dean's expansion, we shall examine in particular this reciprocal pair of Stokes series.

3. Computer extension of Dean's series

Numbers are kept within range on the computer by incorporating the powers of 576 that appear in (2.7) and (2.8) into the expansion, rewriting Dean's series (2.5) as

$$w = \sum_{n=0}^{\infty} (\tfrac{1}{576}K)^n w_n, \quad \psi = \sum_{n=1}^{\infty} (\tfrac{1}{576}K)^n \psi_n. \tag{3.1}$$

By induction we find that the functions w_n and ψ_n depend upon the co-ordinates as follows:

$$\left.\begin{aligned} w_n &= \sum_{i=1}^{I}\sum_{j=1}^{J+1} E_{nij}\begin{cases}\cos(2i-2)\theta\, r^{2j-2}, & n \text{ even}, \\ \sin(2i-1)\theta\, r^{2j-1}, & n \text{ odd}, \end{cases} \\ \psi_n &= \sum_{i=1}^{I}\sum_{j=1}^{J} C_{nij}\begin{cases}\sin(2i-2)\theta\, r^{2j-2}, & n \text{ even}, \\ \cos(2i-1)\theta\, r^{2j-1}, & n \text{ odd}. \end{cases} \end{aligned}\right\} \tag{3.2}$$

Here I and J are the greatest integers less than or equal to $\frac{1}{2}(n+2)$ and $\frac{1}{2}(7n+2)$, respectively. We work also with the corresponding expressions for $\nabla^2 w_n$, $\nabla^4\psi_n$ and $\nabla^2\psi_n$.

† Later writers have mistakenly disputed these coefficients. Adler (1934) claims that the second should be 0·03048, and Sankaraiah & Rao (1973) change the third to 0·012167 without comment; but we have confirmed the second as 1541/50400 = 0·0305754 by hand, and our computer calculations as well as those of Larrain & Bonilla (1970) give the third as 0·01193.

n	a_n	b_n	c_n	d_n	e_n	f_n
0	1·0000000000	1·00000	1·00000	1·00000	1·00000	−0·033237
1	−0·0305753968	0·03058	−0·03162	0·03162	0·01838	0·042766
2	0·0119311827	−0·01100	−0·01886	0·01986	0·00581	−0·006885
3	−0·0065846067	0·00588	−0·01338	0·01461	0·00278	−0·001477
4	0·0042384991	−0·00373	−0·01034	0·01160	0·00161	−0·000530
5	−0·0029771923	0·00259	−0·00840	0·00964	0·00103	−0·000250
6	0·0022124224	−0·00191	−0·00707	0·00826	0·00072	−0·000140
7	−0·0017101745	0·00147	−0·00609	0·00723	0·00052	−0·000089
8	0·0013610001	−0·00117	−0·00534	0·00643	0·00040	−0·000060
9	−0·0011076549	0·00095	−0·00475	0·00579	0·00031	−0·000043
10	0·0009176324	−0·00078	−0·00428	0·00527	0·00026	−0·000031
11	−0·0007712689	0·00066	−0·00389	0·00484	0·00021	−0·000022
12	0·0006560579	−0·00056	−0·00356	0·00447	0·00018	−0·000016

TABLE 1. Coefficients in Stokes series for flux ratio.

We have written a FORTRAN program of some 500 statements that calculates successively the coefficients in these expressions. In outline, it consists of the following segments:

(1) With n even, compute the coefficients of $\nabla^4\psi_n$ from (2.2).
(2) Compute the coefficients C_{nij} of ψ_n.
(3) Compute the coefficients of $\nabla^2\psi_n$.
(4) Increase n by one to become odd, and compute the coefficients of $\nabla^2 w_n$ from (2.1).
(5) Compute the coefficients of w_n.
(6) Return to step 1 with n odd and continue.

Because the program consists mainly of DO loops nested five deep, the computing time is found to increase with between the fifth and sixth powers of the number of terms. The solution was computed up to K^{16} in 8 min on the IBM 360/67 machine, and later up to K^{24} in 5 min on the CDC 7600 machine, which is an order of magnitude faster and has the additional advantage of providing 28 significant figures in double-precision arithmetic. To this order the solution is represented by some 8200 non-zero coefficients C_{nij} in (3.2) and 8900 of the E_{nij}.

Comparison of single- and double-precision computations shows that not quite one significant figure is lost from these coefficients, as a result of truncation and round-off errors, each time n is increased by two. We are therefore confident that our coefficients are all correct to 16 figures.

The coefficients in Dean's series (2.7) for the flux ratio are listed to 10 decimal places in the second column of table 1. Up to $n = 7$ they agree precisely with the results of Larrain & Bonilla (1970) to the seven places that they published. The resulting coefficients for the inverse series (2.8) are given in the third column, but to fewer figures because more can be derived if necessary from those of the direct series.

4. Convergence of Dean's series

Supposing that the critical Reynolds number is the same for a curved as for a straight pipe, Dean (1928) estimated that laminar flow would be of practical interest for values of K up to perhaps 10^5. Remarkably, the experiments of White (1929)

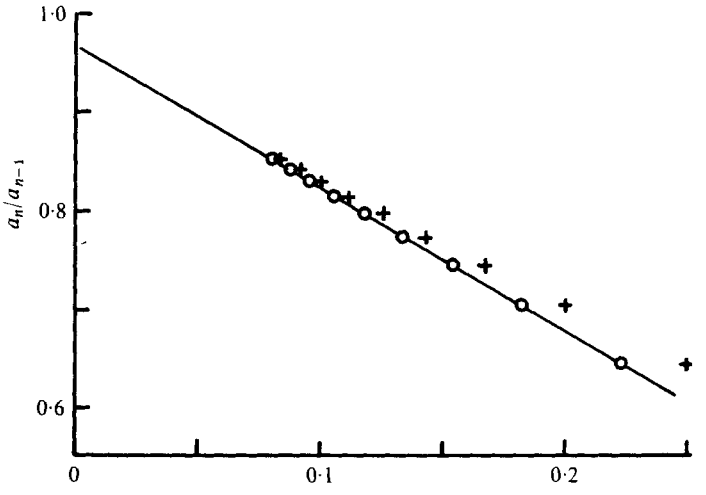

FIGURE 2. Domb–Sykes plot for extended Dean series (2.7). +, plotted *vs.* $1/n$; ○, plotted *vs.* $1/(n+\frac{1}{2})$; ——, asymptote for $\alpha = \frac{1}{2}$ and $\mathscr{R}^{-1} = 0{\cdot}967$.

showed that curvature stabilizes the flow, so that it appeared to be laminar even above $K = 10^6$. On the other hand, Dean suggested that his result is 'probably not valid when K exceeds 400', though he also remarked that the error in (2.7) is not likely to be serious when $K = 576$; and subsequent writers (e.g. Larrain & Bonilla 1970; Sankaraiah & Rao 1973) have concluded that the series converges up to $K = 576$.

We can estimate the radius of convergence $\mathscr{R}$ accurately using a graphical ratio test and other devices for analysing series (Van Dyke 1974; Gaunt & Guttmann 1974). First, we observe that the coefficients in (2.7) alternate regularly in sign; this indicates that the nearest singularity, which limits the convergence, lies on the negative real axis of $(\frac{1}{576}K)^2$. Now if that singularity is algebraic, with exponent α, the ratio a_n/a_{n-1} of successive coefficients will be linear in $1/n$ for large n:

$$\frac{a_n}{a_{n-1}} \sim \frac{-1}{\mathscr{R}}\left(1 - \frac{1+\alpha}{n} + \ldots\right). \tag{4.1}$$

We therefore plot a_n/a_{n-1} *vs.* $1/n$ – the *Domb–Sykes plot* – and fit a straight-line asymptote. Its intercept on the a_n/a_{n-1} axis yields an estimate for the reciprocal of the radius of convergence, and its slope (or the intercept on the $1/n$ axis) indicates the exponent α.

This plot, shown by the crosses in figure 2, is nearly straight, and clearly has an intercept less than unity; thus Dean's series converges for K somewhat greater than 576. Gaunt & Guttmann (1974) point out that a coincident weaker singularity will give a multiple of $1/n^2$ as the next term in (4.1); it can be cancelled, and the Domb–Sykes plot straightened, by a small shift in n. The circles in figure 2 show that plotting *vs.* $1/(n+\frac{1}{2})$ instead of $1/n$ straightens the plot considerably. Fitting a straight line as shown then makes it unmistakably clear that the radius of convergence is

$$(\tfrac{1}{576}K)^2 = (0{\cdot}967)^{-1}.$$

To refine this value, we fit a polynomial of degree N in $(n+\frac{1}{2})^{-1}$ to the last $N+1$ points in figure 2. This is most easily done by forming a *Neville table* of the a_n/a_{n-1},

as described by Gaunt & Guttmann (1974). The terminal slopes amply confirm the square-root singularity to at least five figures, and successively higher-order intercepts on the vertical axis give

$$\mathscr{R}^{-1} \approx 0{\cdot}9670,\ 0{\cdot}96693,\ 0{\cdot}966854,\ 0{\cdot}966861,\ 0{\cdot}966856,\ 0{\cdot}966859,$$
$$0{\cdot}966859,\ 0{\cdot}966858,\ 0{\cdot}966858,\ 0{\cdot}966858,\ 0{\cdot}966858, \ldots. \quad (4.2)$$

To substantiate and further refine this result, we have applied a variety of techniques, including analysis of the inverse series (2.8). These all give consistent results. For example, if we fix the terminal slope to correspond to the square-root singularity and then form a new Neville table, all polynomials in $(n+\frac{1}{2})^{-1}$ of from the seventh to the twelfth degree give $\mathscr{R}^{-1} = 0{\cdot}96685840$. Thus we conclude that Dean's series (2.7) for the flux ratio converges up to

$$(\tfrac{1}{5}\tfrac{1}{7}\tfrac{1}{6}K)^2 = (0{\cdot}96685840)^{-1}, \quad K = 585{\cdot}78878. \quad (4.3)$$

The question is sometimes asked whether the series for other quantities will have the same radius of convergence. It seems plausible that they will; and this was confirmed by analysing the series for four local quantities:

(i) the axial velocity w down the centre of the pipe,

(ii) the transverse velocity across the centre of the pipe,

(iii) the transverse skin friction (or vorticity) at the top of the pipe,

(iv) the gradient of skin friction at the innermost point.

In each case the Domb–Sykes plot is just as smooth as figure 2, and clearly points to the same radius of convergence. The slopes also indicate that the singularity is a square root for each quantity, this agreement arising only because the square root is not the leading term in the expansion about the nearest singularity but is preceded by a constant. Furthermore, Domb–Sykes plots for the limited number of coefficients computed by Larrain & Bonilla (1970) make clear that the radius of convergence is also the same for higher powers of the curvature ratio a/L, whereas the order of the singularity for the coefficient of $(a/L)^m$ is apparently $\frac{1}{2}-m$.

5. Analytic continuation to $K = \infty$

The nearest singularity has no apparent physical significance. We therefore banish it to infinity, and increase the range of convergence for physically significant K by applying an Euler transformation, recasting the series in powers of

$$\epsilon = \frac{(\tfrac{1}{5}\tfrac{1}{7}\tfrac{1}{6}K)^2}{(0{\cdot}96685840)^{-1} + (\tfrac{1}{5}\tfrac{1}{7}\tfrac{1}{6}K)^2}. \quad (5.1)$$

Thus Dean's series (2.7) for the flux ratio becomes

$$F_c/F_s = \sum_{n=0}^{\infty} c_n \epsilon^n = 1 - 0{\cdot}03162\epsilon - 0{\cdot}01886\epsilon^2 - \ldots, \quad (5.2)$$

and the inverse series (2.8) becomes

$$(F_c/F_s)^{-1} = \sum_{n=0}^{\infty} d_n \epsilon^n = 1 + 0{\cdot}03162\epsilon + 0{\cdot}01986\epsilon^2 + \ldots. \quad (5.3)$$

The coefficients c_n and d_n up to terms in ϵ^{12} are given in table 1.

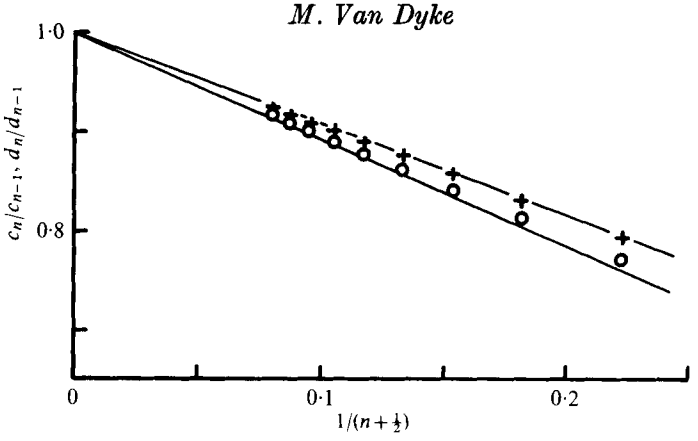

FIGURE 3. Domb–Sykes plots for Dean series after Euler transformation. ○, direct series (5.2); +, inverse series (5.3); ——, asymptotes for $\alpha = \frac{1}{12}$.

The new coefficients have fixed signs, indicating that the nearest singularity now lies on the positive real axis of ϵ. This suggests that, just as for the Oseen drag of a sphere (Van Dyke 1970), we have succeeded in continuing the solution analytically to infinite K, which corresponds to $\epsilon = 1$. This is confirmed by Domb–Sykes plots for the new direct and inverse series (figure 3), and by the associated Neville tables, which show the nearest singularity to lie at $\epsilon = 1$ to within four or five significant figures.

By contrast, estimation of the exponent α of that singularity is a delicate matter, to which we have devoted much effort. Figure 3 makes clear that its value is very small; we show the terminal slopes for the direct and inverse series with $\alpha = \frac{1}{12}$, which is the value according to all the boundary-layer models in the literature. However, the corresponding Neville tables are irregular; and various attempts to substantiate this value, for example by admitting coincident weaker singularities, have invariably led to inconsistencies.

The most glaring inconsistency arises from attempting to estimate the coefficient C of the singularity at $\epsilon = 1$ by *completing* the series (Van Dyke 1974) on the assumption that $\alpha = \frac{1}{12}$, that is, by fitting the Taylor expansion of $C(1-\epsilon)^{\frac{1}{12}}$ to successive terms in the Euler-transformed Dean series (5.2). This yields the sequence of estimates

$$C \approx 1,\ 0{\cdot}379,\ 0{\cdot}494,\ 0{\cdot}548,\ 0{\cdot}581,\ 0{\cdot}603,\ 0{\cdot}618,\ 0{\cdot}631,$$
$$0{\cdot}640,\ 0{\cdot}647,\ 0{\cdot}653,\ 0{\cdot}658,\ 0{\cdot}663,\ \ldots. \quad (5.4)$$

These plot almost linearly *vs.* $1/n$, extrapolating to $C = 0{\cdot}71$. On the other hand, fitting $C^{-1}(1-\epsilon)^{-\frac{1}{12}}$ to the corresponding inverse series (5.3) yields

$$C \approx 1,\ 2{\cdot}635,\ 2{\cdot}273,\ 2{\cdot}146,\ 2{\cdot}083,\ 2{\cdot}047,\ 2{\cdot}025,\ 2{\cdot}010,$$
$$2{\cdot}000,\ 1{\cdot}994,\ 1{\cdot}990,\ 1{\cdot}988,\ 1{\cdot}987,\ \ldots, \quad (5.5)$$

and when plotted *vs.* $1/n$ these extrapolate instead to $C = 1{\cdot}98$.

We have concluded after considerable study that this discrepancy can be resolved only by abandoning the exponent $\alpha = \frac{1}{12}$, and with it the traditional boundary-layer model of Adler (1934) and his successors. In fact, we have determined α by requiring that the completion coefficients for the direct and the inverse series be compatible. Figure 4 shows that their product extrapolates linearly in $1/n$, and tends to unity for $\alpha = \frac{1}{20}$.

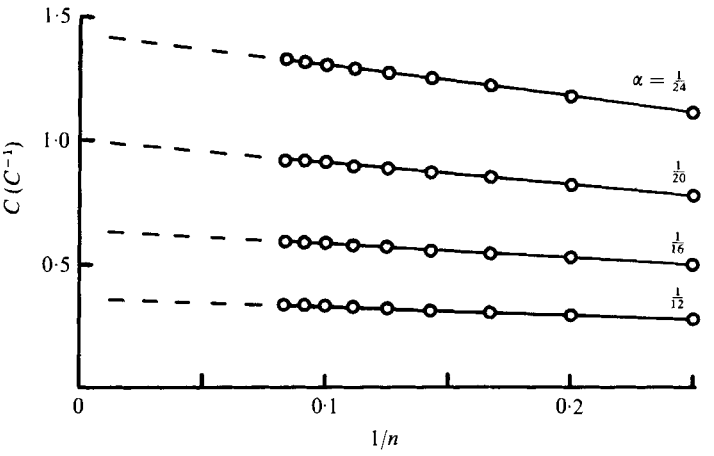

FIGURE 4. Extrapolation of product of completion coefficients for direct and inverse series.

This conclusion is so surprising that we have sought to corroborate it in a number of ways. Of these we mention three devices that were applied to the Euler-transformed series (5.2) and (5.3). First, we applied to the direct and inverse series the technique of 'critical-point renormalization' (Hunter & Baker 1973), which enables one to estimate the difference between the exponents for two different functions known to be singular at the same point. This involves forming a new series for a 'generating function' whose exponent is one less than the difference of the original two exponents. In our case this new exponent is $2\alpha - 1$, and then making a Domb–Sykes plot of the new coefficients, and a Neville table, yields the sequence of estimates

$$\alpha \approx 0{\cdot}0555,\ 0{\cdot}0550,\ 0{\cdot}0535,\ 0{\cdot}0523,\ 0{\cdot}0512,\ 0{\cdot}0503,\ \ldots. \tag{5.6}$$

(We dare proceed no further, though the next value is still closer to $\frac{1}{20}$, because the upper halves of Neville tables have been found generally to be erratic in this problem.)

Second, we show in figure 5 a magnified Domb–Sykes plot with n shifted by the $\frac{1}{2}$ that was found to straighten the plot for the original series (figure 2). The ratios are seen to lie close to the lines for $\alpha = \frac{1}{20}$, and to twine slightly about them: a phenomenon that was encountered in exaggerated form in the corresponding plot for the Oseen drag of a sphere (Van Dyke 1970, figure 2).

Third, we have formed the series for the logarithm of the flux ratio F_c/F_s. Then comparing with the expansion of $\ln(1-\epsilon)^\alpha$ yields the sequence of estimates

$$\alpha \approx 0{\cdot}03162,\ 0{\cdot}03872,\ 0{\cdot}04197,\ 0{\cdot}04384,\ 0{\cdot}04505,\ 0{\cdot}04588,\ 0{\cdot}04649,$$
$$0{\cdot}04694,\ 0{\cdot}04729,\ 0{\cdot}04756,\ 0{\cdot}04777,\ 0{\cdot}04793,\ \ldots. \tag{5.7}$$

Except for the first three, these are fitted to within $\frac{1}{5}$ % by

$$\alpha = \tfrac{1}{20}(1 - 1/2n). \tag{5.8}$$

One might object to $\frac{1}{20}$ as being a rather unlikely exponent. However, we shall see that when converted to quantities appropriate to large values of K it corresponds to an exponent having the more plausible value $\frac{1}{4}$.

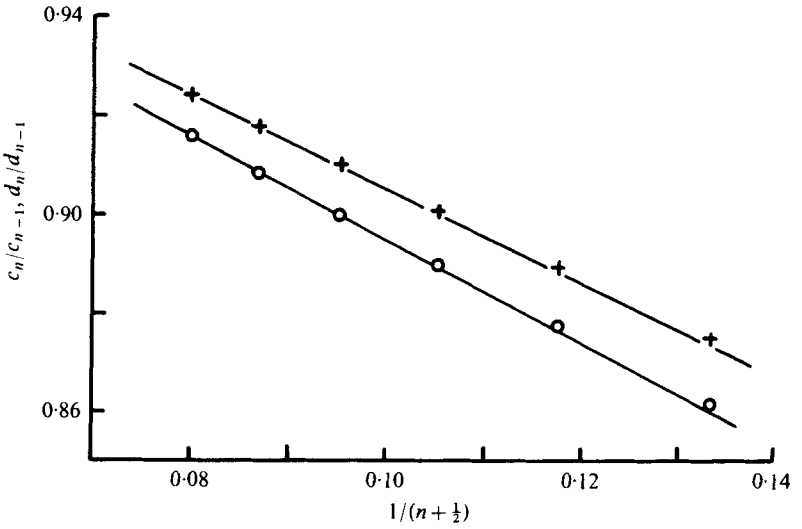

FIGURE 5. Magnified Domb–Sykes plot. ○, direct series; +, inverse series; ——, asymptotes for $\alpha = \frac{1}{20}$.

An independent analysis of the original Dean series (2.7), which does not depend on our estimate (4.3) of its radius of convergence, is provided by Padé approximants. A Padé approximant is the ratio of two polynomials that, when expanded, agrees with a power series to as many terms as possible. Such rational fractions are known to have remarkable properties of analytic continuation (Baker 1965). A Padé approximant can simulate a singularity only by the poles that are the zeroes of its denominator; it is therefore more effective to treat a function with a branch point by first forming the series for its logarithmic derivative. Because we are concerned with the singularity at $K^2 = \infty$, we form the $[N/(N+1)]$ approximants, whose denominators are one degree higher than the numerators. Thus from just three terms of Dean's series (2.7) we form the [0/1] approximant:

$$-\frac{d}{-d(\frac{1}{5}\frac{1}{7}\frac{1}{6}K)^2}\ln\frac{F_c}{F_s} = \frac{0{\cdot}03058}{1+0{\cdot}74987(\frac{1}{5}\frac{1}{7}\frac{1}{6}K)^2} \sim \frac{0{\cdot}04077}{(\frac{1}{5}\frac{1}{7}\frac{1}{6}K)^2} \quad \text{as} \quad K^2 \to \infty. \tag{5.9}$$

The residue 0·04077 at $(\frac{1}{5}\frac{1}{7}\frac{1}{6}K)^2 = \infty$ is to be compared with our estimate $\alpha = \frac{1}{20}$ for the exponent. Likewise, forming the $[\frac{1}{2}]$, $[\frac{2}{3}]$, ..., $[\frac{5}{6}]$ approximants gives

$$\alpha \approx 0{\cdot}04077,\ 0{\cdot}04666,\ 0{\cdot}04821,\ 0{\cdot}04856,\ 0{\cdot}04858,\ 0{\cdot}04867,\ \ldots. \tag{5.10}$$

This sequence is evidently (with the slightly erratic convergence that is typical of Padé approximants) approaching $\frac{1}{20}$ rather than $\frac{1}{12}$.

6. The secondary singularity at $K = \infty$

Convinced that the dominant singularity is a multiple of $(1-\epsilon)^{-\frac{1}{20}}$, we undertake to extract it, and thereby improve the rate of convergence of the series. Multiplicative extraction yields

$$\begin{aligned} F_c/F_s &= (1-\epsilon)^{\frac{1}{20}} \sum_{n=0} e_n \epsilon^n \\ &= (1-\epsilon)^{\frac{1}{20}}(1 + 0{\cdot}01838\epsilon + 0{\cdot}00581\epsilon^2 + \ldots). \end{aligned} \tag{6.1}$$

The first 13 coefficients e_n are listed in table 1.

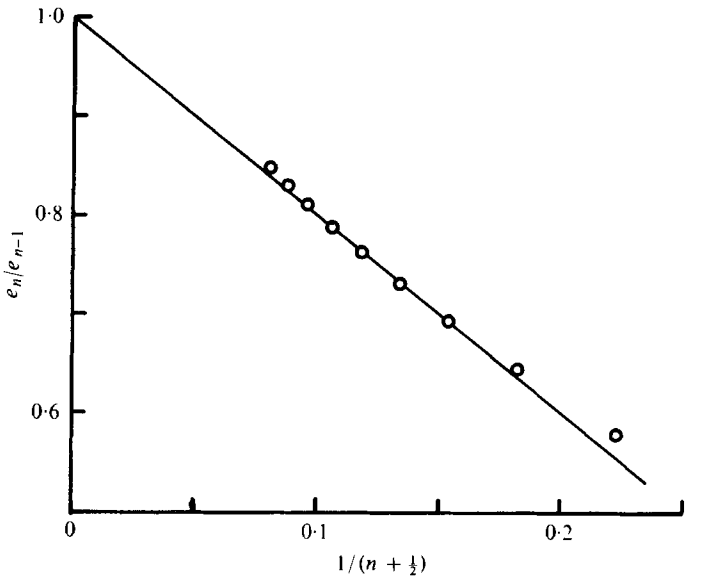

FIGURE 6. Domb–Sykes plot for Dean series after Euler transformation and multiplicative extraction of dominant singularity. ——, asymptote for $\alpha = 1$.

A new Domb–Sykes plot, with n again shifted by $\frac{1}{2}$ (figure 6), shows that the secondary singularity is also located at $\epsilon = 1$. The slope clearly corresponds to the exponent $\alpha = 1$. Such a non-negative integral value indicates that logarithmic terms intervene, in this case a multiple of $(1-\epsilon)\ln(1-\epsilon)$. The same conclusion is a consequence of (5.8), which in fact corresponds to the more definite result

$$F_c/F_s = A(1-\epsilon)^{\frac{1}{20}}[1+\tfrac{1}{40}(1-\epsilon)\ln(1-\epsilon)+\ldots]. \tag{6.2}$$

Evaluating the sum in (6.1) after completing it according to (6.2) gives $A = 1{\cdot}0343$. Thus we recast the series finally as

$$F_c/F_s = 1{\cdot}0343(1-\epsilon)^{\frac{1}{20}}\left[1+\tfrac{1}{40}(1-\epsilon)\ln(1-\epsilon)+\sum_{n=0}^{\infty} f_n\epsilon^n\right], \tag{6.3}$$

where the first 13 coefficients f_n are listed in table 1. A new Domb–Sykes plot oscillates too much to be relied upon, but suggests that the tertiary singularity may be a multiple of $(1-\epsilon)^2\ln(1-\epsilon)$. Further refinement is unnecessary, however, because this last version of Dean's series yields at least four-figure accuracy for all values of K.

Our difficulties in determining the exponent α can now be understood by studying (6.2) as a model. Its expansion in powers of ϵ yields a Domb–Sykes plot that twines about the asymptote just like figure 5, and its Neville table is equally irregular up to the first 13 terms. However, as the number of terms is increased to 20, the exponent $\alpha = \frac{1}{20}$ unmistakably asserts itself. Thus our elaborate analysis in § 5 could probably have been replaced by a simple ratio test if we had been able to extend Dean's series (3.1) to the 40th rather than only the 24th power of K.

K	D	κ	λ_c/λ_s
50	28·28	5·00	1·000
312·5	70·71	12·46	1·008
576	96	16·58	1·024
800	113·14	19·26	1·039
1012·5	127·28	21·40	1·051
4000	252·98	37·98	1·178
15625	500	65·70	1·345
22931	605·72	76·61	1·398
45000	848·53	100·5	1·492
62500	1000	114·4	1·545
80000	1131·37	126·5	1·581
130050	1442·50	153·7	1·660
250000	2000	199·2	1·774
285012·5	2135·46	210·3	1·795
765625	3500	311·8	1·985
877812·5	3747·67	329·8	2·009
1562500	5000	414·7	2·131
2000000	5656·85	458·5	2·181

TABLE 2. Friction factor from modified Dean series (6.3) as function of three variants of Dean number.

7. Comparison with other results for friction ratio

We have worked with the parameter K of Dean, which is convenient for theoretical purposes although it is based on a hypothetical reference speed. Two other versions of the 'Dean number' are in common use in the literature.† McConalogue & Srivastava (1968) introduced a parameter D that is related to that of Dean simply by $D = 4K^{\frac{1}{2}}$. White (1929) introduced an essentially different parameter κ that is more useful in experiment (and also at high Dean number) because it is based on the actual mean velocity $\overline{W}$ down the pipe, according to

$$\kappa \equiv \frac{2a\overline{W}}{\nu}\left(\frac{a}{L}\right)^{\frac{1}{2}}. \tag{7.1}$$

It is therefore related to Dean's K and McConalogue & Srivastava's D through the flux ratio itself, according to

$$\frac{F_c}{F_s} = \frac{\kappa}{(\frac{1}{2}K)^{\frac{1}{2}}} = 2^{\frac{5}{2}}\frac{\kappa}{D}. \tag{7.2}$$

Values of the friction ratio $\lambda_c/\lambda_s = (F_c/F_s)^{-1}$ given by our modified Dean series (6.3) are shown in table 2, together with the corresponding values of D and κ. The values of K chosen are those for which finite-difference solutions are available.

In terms of White's parameter κ, Dean's series (2.7) for the flux ratio becomes

$$F_c/F_s = 1 - 0{\cdot}03058(\kappa^2/288)^2 + 0{\cdot}00819(\kappa^2/288)^4 + \ldots. \tag{7.3}$$

We have seen that this converges for $\kappa < 16{\cdot}7$. To compare with the boundary-layer analyses, we also convert our asymptotic expression to White's parameter. We have

† The notation is confusingly non-uniform; for example, the K of Adler (1934) and Larrain & Bonilla (1970) is our (and Dean's) $\frac{1}{576}K$; the K of Mori & Nakayama (1965) and Itō (1969) is our (and White's) κ; the K of Smith (1976) is our $\frac{1}{2}K$ and his D is our $2^{-\frac{1}{2}}D$; and the N_{De} of Truesdell & Adler (1970) and Austin & Seader (1973), the k of Hasson (1955) and Barua (1963), and the D of Prandtl (1931) are our κ.

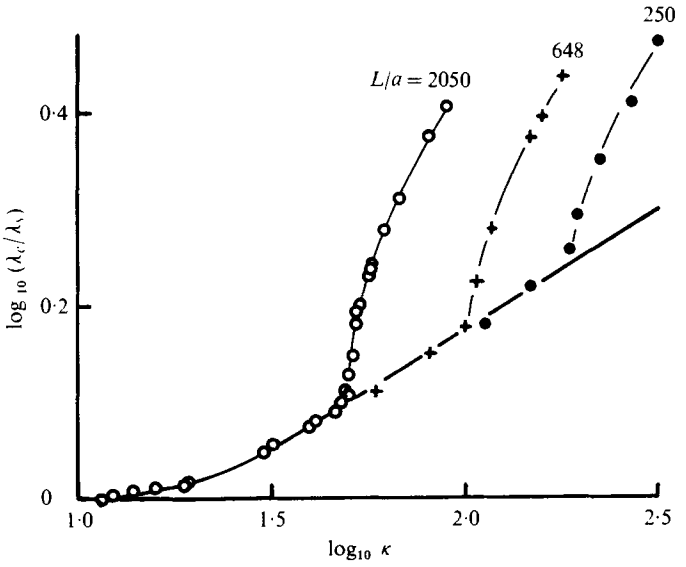

FIGURE 7. Experimental friction ratios for loose coiling. ○, White (1929); +, ●, Itō (1959); ——, present theory.

seen that at high Dean number the flux ratio decreases as $1{\cdot}0343(1-\epsilon)^{\frac{1}{10}}$. In view of (5.1), this means that

$$F_c/F_s \sim 1{\cdot}9562K^{-\frac{1}{10}} \quad \text{as} \quad K \to \infty. \tag{7.4}$$

Combining this with (7.2) yields the asymptotic relationship between White's and Dean's parameters:

$$\kappa \sim 1{\cdot}3833K^{\frac{2}{5}}. \tag{7.5}$$

Hence the flux ratio decays as $2{\cdot}1212\kappa^{-\frac{1}{4}}$, or the friction ratio grows asymptotically as

$$\lambda_c/\lambda_s = (F_c/F_s)^{-1} \sim 0{\cdot}47136\kappa^{\frac{1}{4}}. \tag{7.6}$$

We see from table 2 that this agrees with our complete expression to within 1 % above $\kappa = 30$.

We can now compare our results for the friction factor with previous experiments, boundary-layer analyses and numerical solutions.

Figure 7 shows, in the logarithmic plot introduced by White (1929), a comparison with experiments on pipes with curvature ratios no greater than $\frac{1}{25}$. The agreement is excellent, the measured friction ratios lying on our curve within experimental scatter until they break away sharply at the onset of turbulence. They seem to cover enough of the straight portion to confirm our conclusion that the friction varies asymptotically as $\kappa^{\frac{1}{4}}$.

Figure 8 shows how the situation changes when more tightly coiled pipes are included. The envelope of experimental points, which presumably corresponds to steady laminar flow, then rises continuously above our curve. It is well fitted by the equation

$$\lambda_c/\lambda_s = 0{\cdot}0969\kappa^{\frac{1}{2}} + 0{\cdot}556, \tag{7.7}$$

which Hasson (1955) proposed to correlate White's measurements in the range $30 < \kappa < 2000$.†

† On the other hand, Prandtl (1931) fitted the experiments with $\lambda_c/\lambda_s = 0{\cdot}37\kappa^{0{\cdot}36}$.

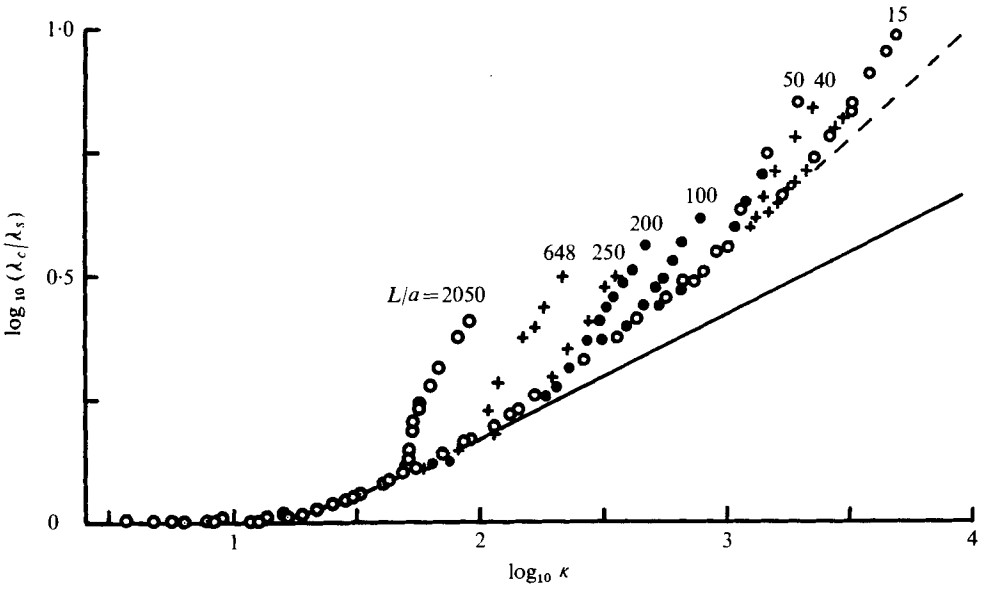

FIGURE 8. Experimental friction ratios for various curvature ratios. ○, White (1929); ●, Adler (1934); +, Itō (1959); ——, present theory; – – –, correlation of Hasson (1955).

A square-root variation with κ is also predicted by all the boundary-layer analyses in the literature. Despite significant differences in the basic assumptions and methods of approximation, they all give practically the same asymptotic result:

$$\frac{\lambda_c}{\lambda_s} \sim \begin{cases} 0{\cdot}1064\kappa^{\frac{1}{2}} & \text{(Adler 1934)}, \\ 0{\cdot}09185\kappa^{\frac{1}{2}} & \text{(Barua 1963)}, \\ 0{\cdot}1080\kappa^{\frac{1}{2}} & \text{(Mori \& Nakayama 1965)}, \\ 0{\cdot}1033\kappa^{\frac{1}{2}} & \text{(Itō 1969)}. \end{cases} \tag{7.8}$$

The results of finite-difference solutions by three different investigators are shown in figure 9. They agree well with our theory up to about $\kappa = 100$, then rise above it in accord with the measurements for tighter coiling, and tend towards the boundary-layer results. In fact, Collins & Dennis (1975) have fitted their values with

$$\lambda_c/\lambda_s = 0{\cdot}1028\kappa^{\frac{1}{2}} + 0{\cdot}380. \tag{7.9}$$

8. Discussion

It is an unexpected result of our analysis that the friction factor in a loosely coiled pipe grows asymptotically as the one-fourth power of the Dean number based on mean axial speed. This conclusion appears to be confirmed by experiments for curvature ratios smaller than $\frac{1}{250}$, whereas more tightly coiled pipes tend towards a square-root variation.

This suggests that the asymptotic behaviour may depend on the manner in which the Dean number tends to infinity. Dean's expansion (2.7) is based on the double limit

$$\left.\begin{aligned} 2a\overline{W}/\nu &\to \infty, \\ a/L &\to 0, \end{aligned}\right\} \quad \kappa \equiv \frac{2a\overline{W}}{\nu}\left(\frac{a}{L}\right)^{\frac{1}{2}} \quad \text{fixed (and small)}, \tag{8.1}$$

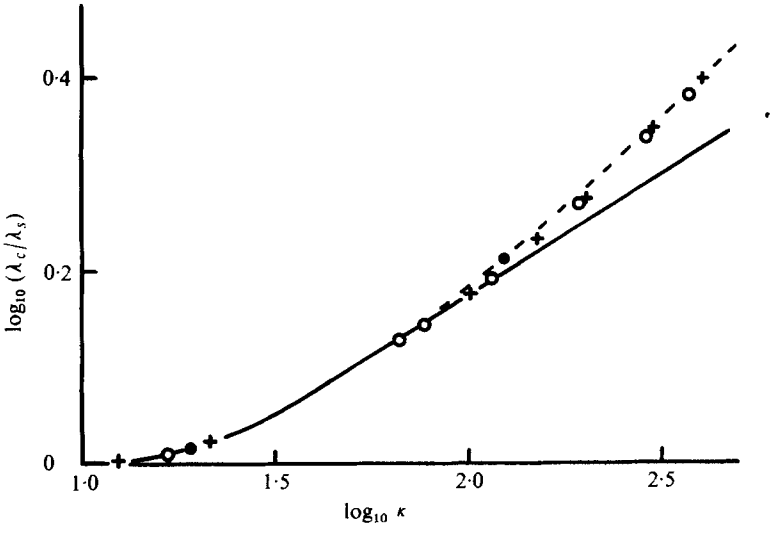

FIGURE 9. Friction ratio from finite-difference solutions. ○, Collins & Dennis (1975), $a/L \to 0$; +, Austin & Seader (1973), $a/L = 0{\cdot}01$; ●, Truesdell & Adler (1970), $a/L = 0{\cdot}01$; ——, present theory; – – –, Hasson's (1955) correlation of experiments.

and we have subsequently extracted the limit $\kappa \to \infty$. On the other hand, flow at high Dean number in a pipe of moderately small curvature ratio would correspond to the single limit

$$2a\overline{W}/\nu \to \infty, \quad a/L \text{ fixed (and small)}. \tag{8.2}$$

An alternative explanation of the departure of the experiments from our curve might be that for more tightly coiled pipes the steady laminar flow is succeeded not by turbulent flow, but by an intermediate regime of unsteady laminar motion, with higher friction. Introducing coloured fluid into the fully developed flow in glass pipes with $L/a = 18{\cdot}7$ and $31{\cdot}9$, Taylor (1929) found that at a certain speed the coloured band began to vibrate in an irregular manner, but retained its identity through at least one whole turn of the helix; and the motion became fully turbulent only at an appreciably higher speed.

However, neither of these explanations can account for the discrepancy in the boundary-layer results, for they are all based on the assumptions of vanishing curvature ratio a/L and steady flow. We conclude that they are incorrect.

The various boundary-layer analyses differ among themselves in basic structure, in particular in the provision that they make for recirculation of the boundary layer that is supposed to flow inward on the walls. Adler (1934) believes that the boundary layers on the two halves of the torus collide at the innermost circle, separate there, and form a re-entrant jet that moves outward through the core; but he makes no attempt to incorporate that phenomenon into his analysis. Likewise, Itō (1969) finds that his boundary-layer solution breaks down in the immediate vicinity of the innermost ring, but does not inquire into the subsequent course of the fluid. On the other hand Mori & Nakayama (1965), believing that collision of the boundary layers is unreasonable, deliberately suppress it. Smith (1975), assuming that a solution with attached boundary layers exists, shows that the velocity would vanish in non-analytic fashion at the innermost circle. Finally, Barua (1963) claims that the boundary layers separate

from the wall at about 27° from the inside, but does not consider how that would alter his assumed core flow.

If the conventional boundary-layer model is wrong, how is it to be corrected? It will apparently contain multiple regions, scaled according to various powers of the Dean number; but we have been unable to devise a consistent structure. In principle, we could extract it from our series; but each local flow quantity has to be analysed by the laborious process described in §§ 5 and 6. We have, however, treated in this way the velocity components at the centre of the pipe. The axial velocity w down the centre (referred to W_0) is found to decay asymptotically as $\kappa^{-\frac{1}{2}}$, just as in the boundary-layer models. On the other hand, the transverse velocity across the centre (referred to ν/a) appears to grow as κ, in disagreement with the $\kappa^{\frac{1}{2}}$ from the boundary-layer theories. This would seem to support Adler's suggestion of a re-entrant jet.

Most of our disagreement with the numerical solutions (figure 9) is also explained if the asymptotic behaviour depends on the limiting process, for the curvature ratio is finite (though small) except in Collins & Dennis's calculations. In any case, it is likely that all the computations suffer from too large a mesh. At the higher Dean numbers, where discrepancies appear, only a few points were used within the boundary layer. In a comparable finite-difference solution for a curved pipe of square cross-section, the calculations of Cheng, Lin & Ou (1976) show the friction ratio increasing approximately as $\kappa^{\frac{1}{2}}$ up to $\kappa = 100$, and thereafter rising much faster; but at just that point the values of the friction evaluated from the pressure gradient and from the wall shear begin to differ considerably, so that both values are suspect.

We conclude that the technique of extending a Stokes series by computer and then analysing and improving it has, in this problem, yielded information that is not accessible by any other method. In fact, the nature of steady fully developed flow in a loosely coiled pipe has been seriously misrepresented by both numerical solutions, which appear to suffer from inadequate mesh refinement at the higher Dean numbers, and boundary-layer analyses, which have all been based on an incorrect model of the flow structure.

This work was supported by the U.S. Air Force Office of Scientific Research under Grant No. AFOSR 74–2649. The author is indebted to Dean Chapman for arranging time on the CDC 7600 computer at the NASA Ames Laboratory, and to John Rakich for patiently and skilfully adapting the program to that machine. He has received valuable advice and encouragement from Andreas Acrivos, George Homsy, Joseph Keller, Niklaus Rott and Leonard Schwartz. He has also benefited from correspondence and discussion with S. C. R. Dennis, William Reynolds and Norman Riley, though he cannot hope that all those colleagues endorse the conclusions reached here.

REFERENCES

Adler, M. 1934 Strömung in gekrümmten Rohren. *Z. angew. Math. Mech.* **5**, 257–275.

Akiyama, M. & Cheng, K. C. 1971 Boundary vorticity method for laminar forced convection heat transfer in curved pipes. *Int. J. Heat Mass Transfer* **14**, 1659–1675.

Austin, L. R. & Seader, J. D. 1973 Fully developed viscous flow in coiled circular pipes. *A.I.Ch.E. J.* **19**, 85–94.

Baker, G. A. 1965 The theory and application of the Padé approximant method. In *Advances in Theoretical Physics* (ed. K. A. Brueckner), vol. 1, pp. 1–58. Academic Press.

BARUA, S. N. 1963 On secondary flow in stationary curved pipes. *Quart. J. Mech. Appl. Math.* **16**, 61–77.

CHENG, K. C., LIN, R.-C. & OU, J.-W. 1976 Fully developed laminar flow in curved rectangular channels. *Trans. A.S.M.E., J. Fluids Engng* **98**, 41–48.

COLLINS, W. M. & DENNIS, S. C. R. 1975 The steady motion of a viscous fluid in a curved tube. *Quart. J. Mech. Appl. Math.* **28**, 133–156.

CONWAY, B. A. 1978 Extension of Stokes series for flow in a circular boundary. *Phys. Fluids* (to appear).

DEAN, W. R. 1927 Note on the motion of fluid in a curved pipe. *Phil. Mag.* (7), **4**, 208–223.

DEAN, W. R. 1928 The stream-line motion of fluid in a curved pipe. *Phil. Mag.* (7), **5**, 673–695.

GAUNT, D. S. & GUTTMANN, A. J. 1974 Series expansions: analysis of coefficients. In *Phase Transitions and Critical Phenomena* (ed. C. Domb & M. S. Green), vol. 3, pp. 181–243. Academic Press.

HASSON, D. 1955 Streamline flow resistance in coils. *Res. Correspondence* **1**, S1.

HUNTER, D. L. & BAKER, G. A. 1973 Methods of series analysis. I. Comparison of current methods used in the theory of critical phenomena. *Phys. Rev.* B **7**, 3346–3376.

ITŌ, H. 1959 Friction factors for turbulent flow in curved pipes. *Trans. A.S.M.E., J. Basic Engng* **81**, 123–134.

ITŌ, H. 1969 Laminar flow in curved pipes. *Z. angew. Math. Mech.* **11**, 653–663.

KUWAHARA, K. & IMAI, I. 1969 Steady, viscous flow within a circular boundary. *Phys. Fluids Suppl.* **12**, II 94–101.

LARRAIN, J. & BONILLA, C. F. 1970 Theoretical analysis of pressure drop in the laminar flow of fluid in a coiled pipe. *Trans. Soc. Rheol.* **14**, 135–147.

MCCONALOGUE, D. J. & SRIVASTAVA, R. S. 1968 Motion of a fluid in a curved tube. *Proc. Roy. Soc.* A **307**, 37–53.

MORI, Y. & NAKAYAMA, W. 1965 Study on forced convective heat transfer in curved pipes (1st report, laminar region). *Int. J. Heat Mass Transfer* **8**, 67–82.

PRANDTL, L. 1931 *Abriss der Strömungslehre.* See English trans. *Essentials of Fluid Dynamics*, p. 168. New York: Hafner, 1952.

SANKARAIAH, M. & RAO, Y. V. N. 1973 Analysis of steady laminar flow of an incompressible Newtonian fluid through curved pipes of small curvature. *Trans. A.S.M.E., J. Fluids Engng* **95**, 75–80.

SMITH, F. T. 1975 Pulsatile flow in curved pipes. *J. Fluid Mech.* **71**, 15–42.

SMITH, F. T. 1976 Steady motion within a curved pipe. *Proc. Roy. Soc.* A **347**, 345–370.

TAYLOR, G. I. 1929 The criterion for turbulence in curved pipes. *Proc. Roy. Soc.* A **124**, 243–249. (See also *Scientific Papers* **2**, 195–200. Cambridge University Press.)

TOPAKOGLU, H. C. 1967 Steady laminar flows of an incompressible viscous fluid in curved pipes. *J. Math. Mech.* **16**, 1321–1337.

TRUESDELL, L. C. & ADLER, R. J. 1970 Numerical treatment of fully developed laminar flow in helically coiled tubes. *A.I.Ch.E. J.* **16**, 1010–1015.

VAN DYKE, M. 1970 Extension of Goldstein's series for the Oseen drag of a sphere. *J. Fluid Mech.* **44**, 365–372.

VAN DYKE, M. 1974 Analysis and improvement of perturbation series. *Quart. J. Mech. Appl. Math.* **27**, 423–450.

VAN DYKE, M. 1975 Computer extension of perturbation series in fluid mechanics. *SIAM J. Appl. Math.* **28**, 720–734.

WHITE, C. M. 1929 Streamline flow through curved pipes. *Proc. Roy. Soc.* A **123**, 645–663.